ISSN: 2229-6948(ONLINE)
DOI: 10.21917/ijct.2023.0435

FABRICATION AND CHARACTERIZATION OF S-BAND COMPACT DUAL MODE CLOSE LOOP MICROSTRIP RESONATOR FILTER

Harsh Dashora[1] and Ugra Mohan Roy[2]
[1]U R Rao Satellite Centre, ISRO, Bangalore, India
[2]M S Ramaiah University of Applied Sciences, India

Abstract

Existing communication systems require efficient, compact and portable microstrip filters so that it contributes in enhancing the performance of communication system. Existing communication at S-band system requires spurious free signal transmission as well as reduced insertion and return loss, improved bandwidth and sharp roll off rate. The stated parameters could be improved through the design of a compact resonator filter. Hence, in this paper the design, development and characterization of a dual mode close loop resonator filter on microstrip structure at S-band is discussed. The proposed resonator filter design exhibits performance improvement in terms of insertion loss (<1 dB), return loss (Better than 12 dB), Bandwidth (>5%), sharp role off as compared to existing filter. Dual mode operation of close loop resonator filter is explained through the time varying field distribution. The size optimization of the designed resonator filter is accomplished without altering electrical parameter. The designed resonator filter has also been fabricated on two different substrates and comparative analysis has been carried out. Finally the realized filters have been characterised for its suitability in space applications.

Keywords:

Microstrip, Resonator, Dual Mode, Perturbation, Cavity, Coupling, Transmission Zero

1. INTRODUCTION

The microstrip technology based filters at S-band are designed using distributed microstrip and stripline based components [1]-[4] and deployed in various space application. For the design of a compact close loop resonator filter at S-band the parameters such as Dielectric constant, Frequency, Bandwidth, Insertion loss and Dimension plays a significant role. Due to need of continuous improvement in S-band communication system especially in terms of insertion loss, return loss, bandwidth and roll off rate, we propose the design of compact dual close loop resonator filter. To accomplish that following work has been proposed and carried out.

- Dual mode operation is explained through mathematical expression as well as the field pattern in the resonator.
- Band pass filter at S-band frequency that involves simulation, miniaturisation, optimization, physical implementation and characterisation is discussed.
- The fabricated filter is characterised at various environmental conditions.
- Comparative analysis of simulation results has been carried out.
- Comparative analysis of fabricated filter on different substrates is discussed at specified temperature range.

Designing filter using resonator is trending now a days due to the reason of steep roll off at cut off and almost flat response at pass band, which results into approximately ideal band pass filter. These resonators can be implemented in various methods e.g. waveguide, Substrate Integrated Waveguide (SIW), Stripline and microstrip etc. Further microstrip based resonators itself can be designed in various shapes such as circular, square, ring, triangular, patch etc. They behave as waveguide cavity resonator by considering top and bottom surface as electrical wall and sides as magnetic walls [4]-[7]. A square patch cavity resonator is basically a close loop resonator with dimension of $\lambda_g/2$. If the resonator is converted into other types of shapes such as circular or square then the dimension is λ_g/π and $\lambda_g/4$ respectively [3] [4].

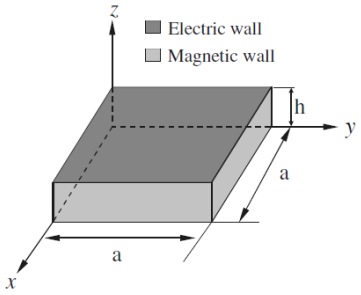

Fig.1. Microstrip based cavity resonator

The resonant frequency of the cavity resonator [8-9] as shown in Fig.1 is given as Eq.(1).

$$f = \frac{1}{2\pi\sqrt{\mu\varepsilon_{eff}}}\sqrt{\left(\frac{m\pi}{a}\right)^2+\left(\frac{n\pi}{a}\right)^2} \quad (1)$$

where, a is effective width of cavity, ε_{eff} is effective permittivity and μ is permeability.

The basic working principle of loop resonator is to establish standing wave across the circumference. Hence phase shift across the loop is integer multiple of 2π as given by equation (2).

$$\beta_l = 2\pi N \quad (2)$$

where, N is integer number and β is phase constant.

The frequency of operation is determined by Eq.(3).

$$f = \frac{v_p}{\lambda} = \frac{Nv_p}{l} \quad (3)$$

where, f is resonant frequency, v_p is phase velocity, λ is wavelength and l is circumference of the loop. In dual mode operation two degenerate modes are employed together to improve filter characteristic. When dual mode operation is used then number of resonators required is half which results into simple and small circuit [4]. There is an additional advantage of using dual mode operation that it enables the resonator to work as doubly tuned network which increases bandwidth [6]. As per the Eq.(1) there are infinite numbers of resonant frequencies available for displayed cavity mode. But there is requirement of two such

modes where electric field pattern is different but resonant frequency is same that is called degenerate modes. Frequency of degenerate mode is given as:

$$f_{100} = f_{010} = \frac{1}{2a\sqrt{\mu\varepsilon_{eff}}} \quad (4)$$

The Eq.(4) shows that field pattern of these degenerate modes is orthogonal to each other. In order to operate the resonator in dual mode condition there is need to couple both the modes hence a perturbation element is placed at line of symmetry of input/output feed lines [10]. A perturbation element is a small patch, notch or cut on the path of field distribution which disturbs the field distribution in microstrip resonator. The placement and size of perturbation is very important to fix the location of transmission zeros (TZ) in filter response [5]. Various work related to these has been demonstrated in the literature. Design of narrow band compact resonator filter using dual mode operation with two coupled degenerate modes has also been reported in [4]. Dual mode filter is generally used for increasing the bandwidth. In order to couple two modes, a perturbation element is used and the size and shape of perturbation element is deciding factor for filter response such as Chebyshev, elliptic etc. [5]-[7]. Filter response consists of two Transmission Zeros (TZ) in both sides of pass band and the placement of TZ is calculated through even mode and odd mode analysis [3]-[4] and the location of TZ can be fine-tuned by altering the size and shape of perturbation element. The principle of close loop resonator is detailed in [11] where S-band filter is designed on Alumina substrate. The fabrication processes for physical implementation on Alumina is detailed in [12]. Before designing any microstrip circuit, the selection of substrate is very important [13] [14]. Testing requirement for the realised using special type of test jig is detailed in [15] and to qualify the prototype for space based application characterisation in various temperature condition needs to be done as detailed in [16]-[18]. Triple-mode band pass filter using a closed loop resonator with periodic stepped-impedance ring resonator (PSIRR) band pass has been reported and results shoes that area miniaturization area and desirable upper stop band is achieved [19] [20]. A stub loaded closed loop microstrip line filter for Wi-Fi applications and a dual-mode defected ground structure resonator is also reported in the literature [21] [22]. At the same time a novel band pass filter with dual-mode open-loop and a compact dual-mode open loop microstrip resonators and filters with improved performance has been reported [23] [24]. Miniaturization plays significant role in the design of resonator. Hexagonal open-loop resonators with E-shaped stubs loading provides miniaturization with improved performance [25]. Recently a novel S-band band pass filter (BPF) with extremely broad stop band and a compact folded band pass filter in empty substrate integrated coaxial line at S band is also reported in the literature [25] [26]. All the existing literature shows that there is need to improvise Bandwidth, Insertion loss, Return loss and Dimension of the S-band filters especially for space applications.

The remaining part of the paper is organized as follows. Section 2 describes the design and simulation of the compact dual mode close loop resonator filter. In section 3 we provide hardware implementation. And in section 4 characterization of the designed filter has been carried out. In section 5, we present the environmental testing of the developed compact close loop filter resonator followed by comparative analysis in section 6. Finally we give concluding remarks and suggest some future work in section 7.

2. DESIGN AND SIMULATION

The filter is designed with specification of centre frequency 2200 MHz, fractional bandwidth 5% and pass band ripple <0.5 dB using ADS commercial simulation software. All the dimensions are measured in mm and simulation results are verified in momentum simulation. The circumference of the square loop is integer multiple of guided wavelength, and is given as Eq.(5).

$$\lambda_g = \frac{\lambda_0}{\sqrt{\varepsilon_{eff}}} \quad (5)$$

In this case, microstrip line width is 1.14 mm and substrate height is 1.25 mm, W/H ratio is 0.912 hence the condition W/H <1 is satisfied and formula for effective dielectric constant is given as:

$$\varepsilon_{eff} = \frac{\varepsilon_r + 1}{2} + \frac{\varepsilon_r - 1}{2}\left[\frac{1}{\sqrt{1+12(H/W)}} + 0.04\left\{1-(H/W)\right\}^2\right] \quad (6)$$

Hence, effective dielectric constant is 6.82 for ε_r = 10.2, guided wavelength is 52.12 mm and characteristic impedance is 50.4 Ω.

Initially the filter is designed with diamond shape of close loop resonator with circumference of λ_g which is further miniaturised by meandering of lines. In this work a novel feeding technique is used where feed lines are connected at two adjacent corners of a square loop which provides minimum distance between two ports is $\lambda_g/4$ and in another path the distance between input/output ports is $3\lambda_g/4$ hence same fosters the orthogonal feed to achieve symmetric filter response [6] as mentioned in Fig.2. Further the loop is rotated by 45 degree for providing input/output ports in same line as shown in Fig.3.This is a novel feeding technique as most of the literatures use feed lines at centre of the edges [4]-[6], [8]-[12].

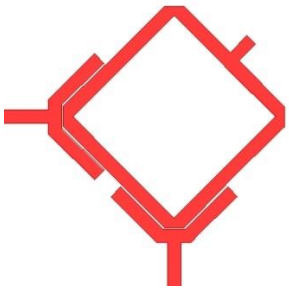

Fig.2. Diamond shaped filter

To achieve the dual mode operation a specific size of perturbation element is used at 135 degree rotation of feed line [11]-[12] which is at diagonal symmetry of the loop. Subsequently optimization is carried out in the topology displayed in Fig.2 and once the desired specification is achieved the filter is modified to improve the common drawback of close loop resonator filter i.e. orthogonal feed lines which is undesirable in

some of the applications. Providing inputs through inline feed by rotating the resonator loop by 45˚ is displayed in Fig.3.

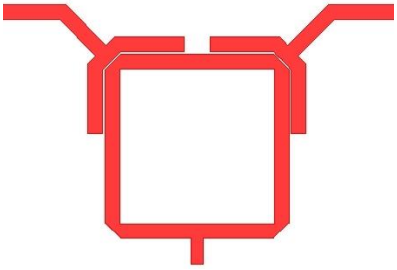

Fig.3. Diamond filter to square filter conversion with inline feed

When perturbation element is not used in the resonator then filter works on single mode. The single mode filter layout with field pattern is given in Fig.4, where a complete cycle of field distribution in single mode operation is detailed.

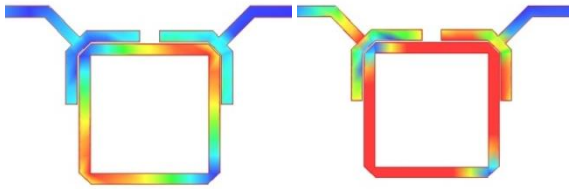

(a) 0˚phase (b) 90˚ phase

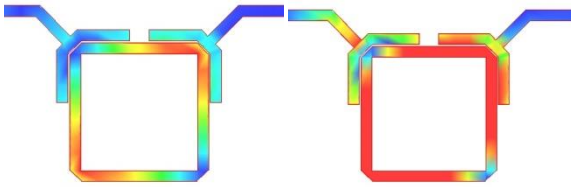

(c) 180˚ phase (d) 270˚phase

Fig.4. Field distribution (A/m) over one cycle of oscillation in single mode operation

In Fig.4, highest field strength is represented in red colour and smallest field strength is represented in blue colour. In Fig.4, it is evident that field strength is oscillating with time in one of the diagonal of square loop.

To understand dual mode operation, two degenerate modes are identified and same is coupled with each other. In order to couple both modes a defect or notch is placed on the resonator loop, called as perturbation element. Perturbation element establishes two split resonant at frequencies at 2200 MHz and 2250 MHz and the field distribution of both modes has 45˚ offset and same is explained in the field pattern of Fig.5. The coupling coefficient between both resonant modes is calculated by Eq.(7) below:

$$K = \frac{f_{02}^2 - f_{01}^2}{f_{02}^2 + f_{01}^2} \quad (7)$$

where f_{01}, f_{02} are known as resonant frequencies of mode-I and mode-II and K is coupling coefficient.

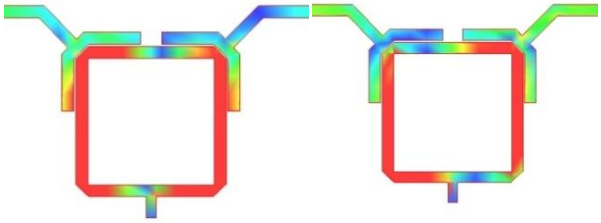

(a) Field pattern in mode-I (b) Field pattern in mode-II

Fig.5. Field pattern of dual mode filter in mode-I (2.20 GHz) and mode-II (2.25GHz)

In Fig.5, it is clearly seen that red colour zone (Peak level of the field) in mode-I and mode-II has shift of 45˚ which provides coupling of two mode in such a way that the field gets distributed across the loop. Field distribution for dual mode filter over the time is detailed in Fig.6.

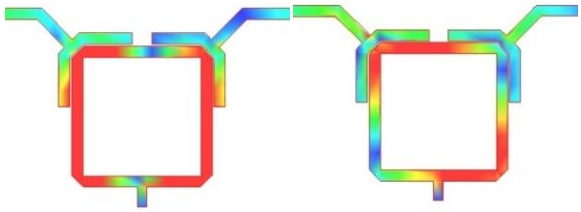

(a) 0˚ phase (b) 45˚phase

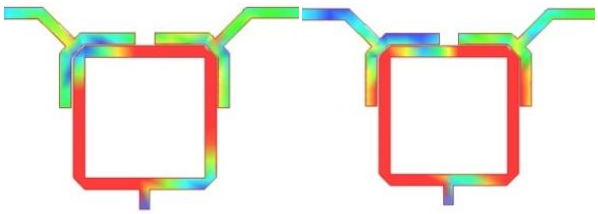

(c) 90˚phase (d) 135˚phase

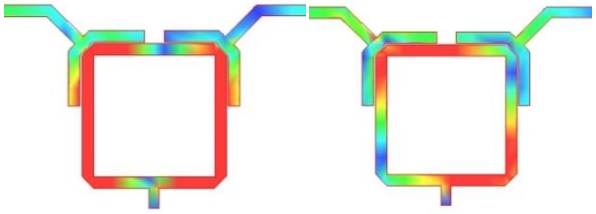

(e) 180˚phase (f) 225˚phase

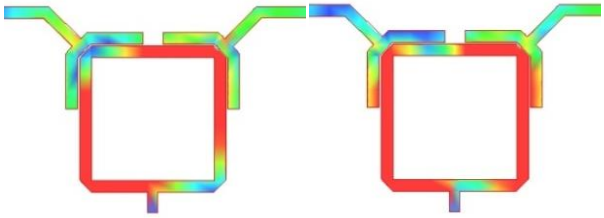

(g) 270˚phase (h) 315˚phase

Fig.6. Field pattern of dual mode filter on different phase angle

In Fig.6, red colour represents highest field strength and blue colour represents minimum field strength. It is seen that as the

phase increases from 0˚ to 360˚, the red colour zone i.e. highest field strength rotates clockwise, which leads to a uniform field or current distribution across the resonator while passing through a complete cycle of wave propagation. The reason behind the field pattern rotation is the 45˚ phase shift between mode-I and mode-II. The phenomenon of coupling of modes through perturbation element can be visualized.

The equivalent circuit of dual mode resonator filter is shown in Fig.7.

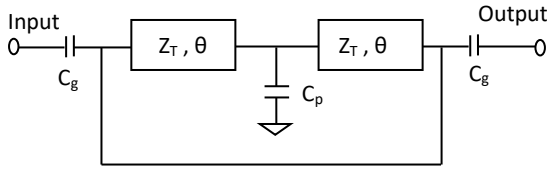

Fig.7. Equivalent circuit of dual mode resonator filter

In Fig.7, Z_T is characteristic impedance of the loop resonator, θ is quarter wavelength in phase form, C_g is gap capacitor at input/output coupling, C_p capacitance of the patch element.

In order to carry out the even-odd mode analysis of the circuit shown in Fig.7, there is requirement of an imaginary electrical wall at line of symmetry that is passing through the patch and mid of the feed lines for even mode analysis. Similarly for odd mode analysis a magnetic wall to be imagined at the line of symmetry as detailed in Fig.8.

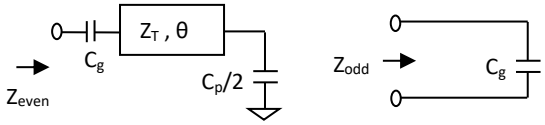

Fig.8. Even mode and odd mode equivalent circuits

In Fig.8, Z_{even} and Z_{odd} is even and odd mode input impedances, respectively. The same is given as Eq.(8) and Eq.(9).

$$Z_{even} = -jZ_T\cot\theta + Z_{cg} + Z_{cp} \quad (8)$$

$$Z_{odd} = Z_{cg} \quad (9)$$

Though the dimension of the filter is reduced to less than half (33x25 mm^2) compared with conventional coupled line filter (70x25 mm^2) [3], still there was a scope for size reduction, hence meandering of microstrip line of the resonator loop is carried out that resulted into further reduction in size up to 24x18 mm2 as shown in Fig.9.

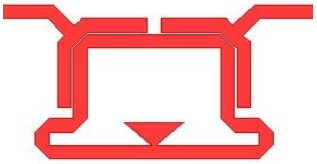

Fig.9. Compact resonator filter at 2.2 GHz

The Fig.9 shows that the perturbation patch is moved inside the loop unlike Fig.3 and shape of the patch is also changed into triangular shape in order to achieve more capacitance that shifts Transmission Zero (TZ) away from the centre frequency [6]. The simulation result is shown in Fig.8.

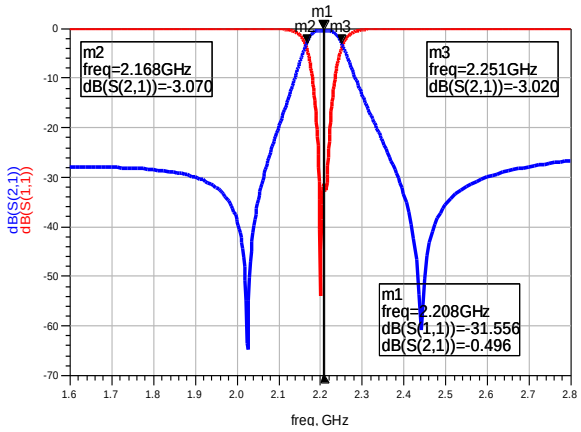

Fig.10. Simulated filter response of Compact resonator filter

In filter response of Fig.10, centre frequency 2208 MHz with fractional bandwidth of 4%, insertion loss of 0.5 dB, return loss of 31 dB and the transmission zeros are observed at 2021 MHz and 2442 MHz which shows excellent selectivity similar to Quasi-elliptic type response.

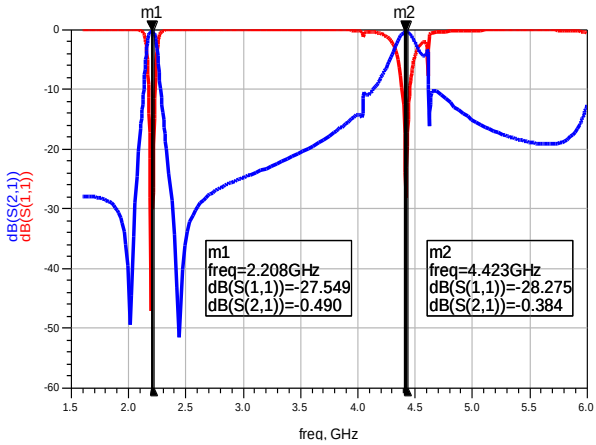

Fig.11. Wide band response of designed filter

The Fig.11 shows the wide band performance of dual mode band pass filter, where it is observed that fundamental pass band response is very close to the ideal filter response and meets all the desired specifications such as insertion loss -0.5 dB and return loss -27.5 dB in pass band. In Fig.11, a second harmonic pass band is also present at 4.42 GHz where insertion loss and return loss is at such level that any signal may pass easily. The reason for second spurious response is due to presence of non-synchronous velocities of even and odd mode operation in dielectric medium [13]. Hence it is advised that applications to be chosen in such a way that no spurious component strikes at that frequency.

3. HARDWARE IMPLEMENTATION

The design is fabricated on two different type of substrates namely RT/Duriod with ε_r = 10.2, tanδ= 0.002, substrate height= 50 mil, copper thickness = 35um and Alumina with ε_r = 9.8, tanδ = 0.001, substrate height = 50 mil, copper thickness= 35um)as detailed in [14]. The chosen parameters are as per the suitability of space environment. Fabrication of prototype on two different

substrates needs two different processes namely photo-lithography process for RT/Duriod (soft substrate)and MIC fabrication using thin film process for Alumina (hard substrate) [12]. Following flow diagram shows that process step of the photo-lithography process and MIC fabrication process:

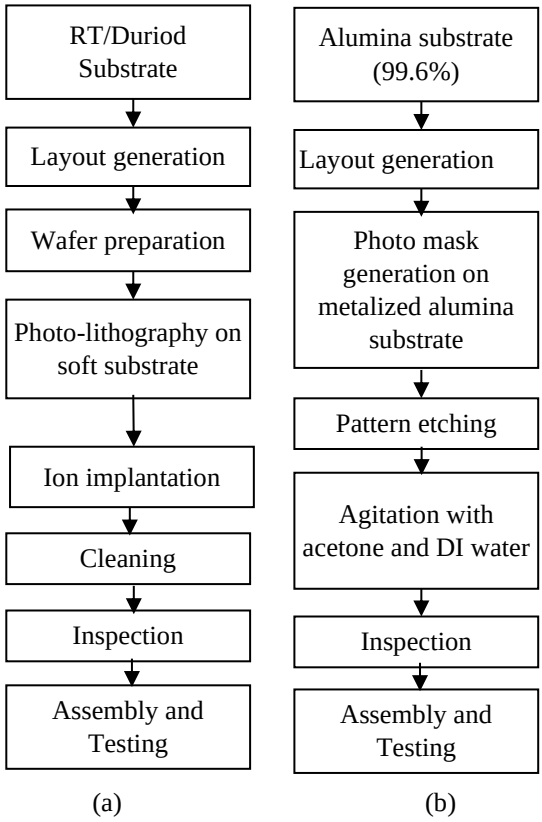

Fig.12. Process flow of PCB fabrication on (a) Soft substrate (RT/Duriod) (b) Hard substrate (Alumina)

In Lithography process the fabricated PCB has Tin plated copper tracks whereas MIC fabrication has gold plated copper tracks, hence conductivity is better in MIC based filter. The fabricated filter on RT/Duriod is shown in Fig.13, whereas the fabricated filter on Alumina is shown in Fig.14.

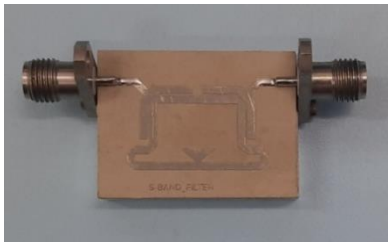

Fig.13. Fabricated filter on RT/Duriod

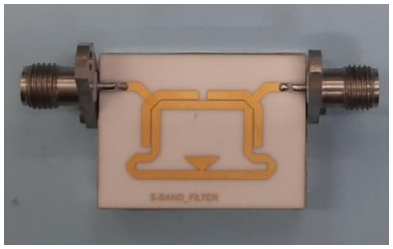

Fig.14. Fabricated filter on Alumina

4. CHARACTERIZATION

The realised filter prototypes on Alumina substrate and RT/Duriod substrate are mounted on suitable test jigs as detailed in [15] for better signal integrity and characterised using Keysight Vector Network Analyzer to measure its performance. The Filter characterisation using Vector Network Analyzer has been shown in Fig.15.

Fig.15. Filter characterisation using Vector Network Analyzer

The Fig.16 and Fig.17 exhibit insertion loss and return loss performance in terms of S_{21} and S_{11} parameters for two different substrate materials.

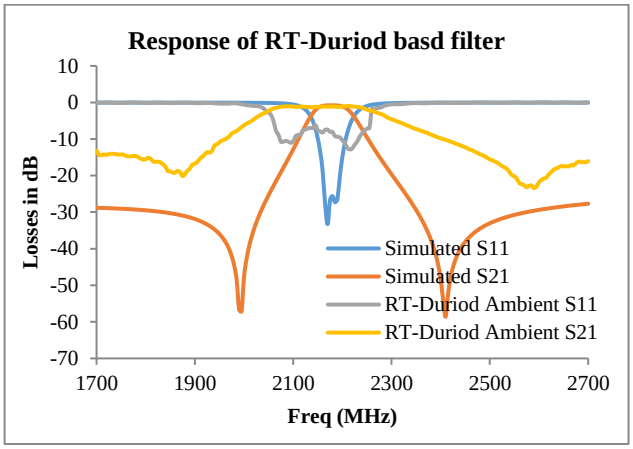

Fig.16: Insertion loss and return loss in RT/Duriod based filter

In Fig.16, simulated results and actual results of RT/Duriod based filter is displayed where actual insertion loss is 0.96 dB, return loss is 12.8 dB and 3-dB bandwidth is 265 MHz with two transmission zeros present at both sides of pass band. The performance of the filter is degraded after fabrication compared to the simulated results. The reason behind this outcome is due to the substrate property, if loss tangent increases, the notch of the curve or depth of transmission zero decreases as detailed in [16] leads to spread the pass band, at the same time soft substrates are in-homogenous sometimes which deteriorates the performance. Apart from that the fabrication process also generates tolerances.

When Alumina based filter is characterised and compared with simulated results as shown in Fig.17, it is observed that both sides of pass band two transmission zeros are present and very good match is there between simulated and actual results. The actual insertion loss is 0.8 dB, return loss is 13.9 dB and 3-dB bandwidth is 160 MHz.

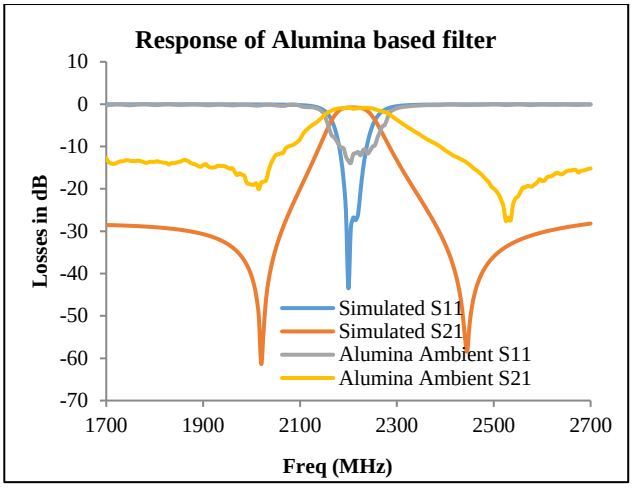

Fig.17. Insertion loss and return loss in Alumina based filter

Deviation is observed in simulated and fabricated results in terms of roll off which is caused due to the fabrication process involved and due to inherent material property of substrate. TR/Duriod 6010 is a soft substrate and there is in-homogeneity observed in dielectric constant across *x* and *y* direction of the substrate. Further the RF connectors are soldered with limited mounting space which led to increased return loss.

5. ENVIRONMENTAL TESTING

In order to ensure the flightworthiness of the designed filter for space applications, same has to undergo with certain environmental tests to get exposure of extreme temperature in space. There are three categories of satellites based on the orbit namely Geostationary Satellite Orbit (GEO), MEO Medium Earth Orbit (MEO) and Lower Earth Orbit (LEO). Based on the height from the earth or orbit, the maximum and minimum temperature experienced by the internal systems of a satellite is estimated. The temperature range for testing the subsystems of the satellite is determined by increasing the temperature range by 5%, 10% or 15% for acceptance level test, proto-flight or qualification level test [18].

In this case the prototype is developed for Indian remote sensing satellite which is a LEO satellite and the temperature range specified for ground testing is -10˚C to +50˚C. Hence both prototypes are characterized for temperature range -10˚C to +50˚C and results are plotted as shown in Fig.18.

The Fig.18 shows that there is a shift in pass band from left to right as the environmental temperature is increased. The centre frequency observed at -10˚C, +25˚C and +50˚C is 2137 MHz, 2170 MHz and 2182 MHz respectively, whereas minimal change in insertion loss and return loss.

In Fig.19, it is observed that there is no change in insertion loss, return loss and centre frequency across the temperature range from -10˚C to +50˚C. Hence it is concluded that, if large temperature variation is experienced by the system then, filter on Alumina can provide consistent performance rather than RT/Duriod based filter for the tested temperature range from -10˚C to +50˚C.

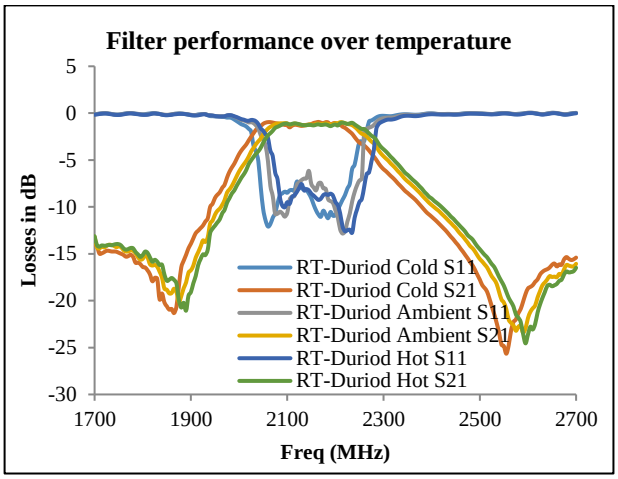

Fig.18. Insertion loss and return loss in RT/Duriod based filter

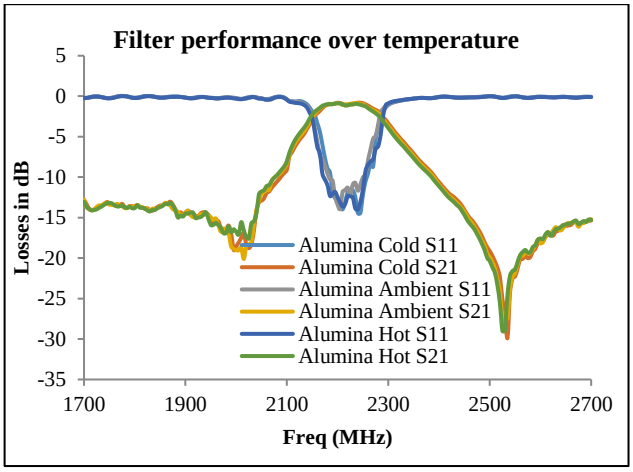

Fig.19. Insertion loss and return loss in Alumina based filter

6. COMPARATIVE ANALYSIS

Both prototypes are compared as discussed in Table.1.

Table.1. Performance Comparison

Parameter	Alumina Substrate		RT/Duriod Substrate	
	Simulated	Actual	Simulated	Actual
Centre freq. (MHz)	2210	2220	2180	2170
Insertion loss (dB)	0.5	0.8	0.78	0.96
Return loss (dB)	-20	-13.9	-26	-12.8
Q-factor	24	13.8	24.4	8.2
Bandwidth (MHz)	100	160	90	265
Roll off (dB/Oct)	-721	-334	-721	-275
Group delay (ns)	-	4.3	-	2.5

Table.2. Performance comparison among the available literatures

Reference	Dielectric constant	Freq (GHz)	BW	Insertion loss (dB)	Return loss (dB)	Dimensions (mm X mm)	Area (mm^2)
[19]	3.0	2.4	4%	2.7	20	35x30	1050
[20]	10.2	1.85	8%	1.7	20	24x30	720
[21]	4.4	2.48	18%	2	15	30x30	900
[22]	3.5	2.57	15%	1.12	20	30x15	450
[23]	3.66	2.4	16.7%	0.5	20	32x14	448
[24]	2.2	1.35	5%	3	15	40x30	1200
[25]	9.8	2.14	2.8%	2	15	18x18	328
[26]	3.55	3	66%	0.8	15	45x12	540
[26]	1	3	2%	3.14	20	52x53	2756
This work	**10.2**	**2.2**	**7%**	**0.9**	**12**	**28x21**	**588**

The Table.1 shows the comparative analysis of simulated and actual results for both type of substrates namely Alumina and RT/Duriod. The comparison indicates that in Alumina substrate insertion loss, return loss and roll off is better (i.e. 0.8 dB, -13.9 dB and -334 dB/Oct respectively) than RT/Duriod substrate which is 0.96 dB, -12.8 dB and -275 dB/Oct respectively but bandwidth and group delay in RT/Duriod is better such as265 MHz and 2.5 ns respectively whereas in Alumina substrate 160 MHz and 4.3 ns respectively. Overall there is very good agreement between simulated and actual results. The actual Fractional Bandwidth (FBW) achieved in alumina-based filter is 7.2% and actual FBW in RT/Duriod based filter is 12.2% which is great advantage extracted by dual mode operation but the actual bandwidth is more than simulated results due to inhomogeneous substrate property particularly in soft substrates. Hence the research work is accomplished with desired outcomes.

Further a comparative analysis is carried out in Table.2 for the recent filter designed at S-band frequency in literatures. The main parameters considered are operating frequency, bandwidth, insertion loss, return loss, dielectric constant and dimension.

7. CONCLUSION

We conclude that close loop dual mode resonator has two degenerate modes. The modes are coupled with each other to achieve the advantages of dual mode operation such as increased bandwidth and sharp roll off. The dual mode operation is explained using electromagnetic field patterns and filter is optimized to get best performance. Initially a diamond shape resonator is used for designing, where signals are fed from corners of the square loop, then the design is modified to get inline feed points, which is further miniaturised to get minimum surface area of 24X18 mm2 and same is successfully demonstrated. The design is fabricated on two different substrates namely RT/Duriod and Alumina, which results as fractional bandwidth of 7.2% on Alumina and fractional bandwidth of 12.2% on RT/Duriod with insertion loss less than 1 dB and return loss of 13 dB. The designed filters have been characterised in different environmental conditions and performance is compared. The design filter is qualified for space-based applications.

8. FUTURE WORK

In this work bandwidth is increased using dual mode operation but in future bandwidth may be increased further using triple mode or quadruple mode operation. Suppression of higher order harmonics may be addressed in future. Further overall performance improvement may be attempted through Defected Ground Structure (DGS), Defected Microstrip Structure (DMS) etc.

ACKNOWLEDGMENT

The authors hereby acknowledge the support and motivation from ISRO-URSC, Bangalore for successful completion of this work. Also sincerely acknowledges HMC and PCB fabrication facility at URSC for their kind support. Authors express sincere gratitude to group directors of Systems Engineering Groups for motivation towards this work with valuable inputs.

REFERENCES

[1] Ramesh Garg, "*Microstrip Line and Slotline*", 3rd Edition, Artech, 2013.
[2] Thomas H. Lee, "Planar Microwave Engineering: A Practical Guide to Theory, Measurement, and Circuits", Cambridge University Press, 2004.
[3] David M. Pozar "*Microwave Engineering*", John Wiley and Sons, 2010.
[4] Jia Sheng and M.J. Lancaster, "Microstrip Filters for RF/Microwave Applications", *John Wiley and Sons*, pp. 235-272, 2001.
[5] R.R. Mansour, "Design of Superconductive Multiplexers using Single-Mode and Dual-Mode Filters", *IEEE Transactions on Microwave Theory and Techniques*, Vol. 42, No. 7, pp. 1411-1418, 1994.
[6] K.G. Avinash and I. Srinivasa Rao, "Compact Dual-Mode Microstrip Bandpass Filters with Transmission Zeros using Modified Star Shaped Resonator", *Progress in Electromagnetics Research C*, Vol. 71, pp. 177-187, 2017.

[7] J. Rao, H. Guo, J. Ni, J. Hong and P. M. Iglesias, "C-Band Microstrip Lossy Filter using Resistive-Loaded Closed-Loop Resonators", *Proceedings of European Conference on Microwave*, pp. 360-363, 2019.

[8] L.A. Rodríguez-Meneses, C. Gutiérrez-Martínez, J. Meza Perez, J.A. Torres Fortiz and R.S. Murphy Arteaga, "Design and Construction of Dual-Mode Micro-Strip Resonator Filters for the 950-1,450 MHz Band: Application as IF Filters in Microwave Transceivers", *Proceedings of IEEE Latin American Symposium on Circuits and Systems*, pp. 1-4, 2021.

[9] A. Arbelaez, "Compact Closed-Loop Resonator Filters with Wide Spurious Free Band and Extended Common-Mode Noise Suppression", *IET Microwaves, Antennas and Propagation*, Vol. 14, No. 9, pp. 860-866, 2020.

[10] S. Aiswarya, S. Bhuvana Nair, L. Meenu and S.K. Menon, "Analysis and Design of Stub loaded Closed Loop Microstrip Line Filter for Wi-Fi Applications", *Proceedings of IEEE International Conference on Wireless & Optical Communication Networks*, pp. 1-5, 2019.

[11] H. Dashora and J. Kumar, "Designing of Miniaturised Dual Mode Resonator Filter for S-Band Frequency", *Proceedings of International Conference for Convergence in Technology*, pp. 1-4, 2021.

[12] Jitendra Kumar, "RF Circuit Realisation using Thick Film Technology", *ICTACT Journal on Microelectronics*, Vol. 7, No. 2, pp. 1115-1120, 2021.

[13] Chandrakanta Kumar, V V Srinivasan, V K Lakshmeesha and S Pal, "Suppression of Second Spurious Pass Band of Hairpin Filter using λg/4 Impedance Transformer", *Proceedings of IEEE International Symposium on Radar*, pp. 1-6, 2007.

[14] H. Dashora, J. Kumar and D. Mamatha, "Effect of Dielectric Substrate and Substrate Selection at Microwave Frequencies", Proceedings of IEEE International Conference on Technology, Engineering, Management for Societal Impact using Marketing, Entrepreneurship and Talent, pp. 1-4, 2020.

[15] Harsh Dashora, Jitendra Kumar and D. Mamatha, "Test Platform for RF Systems and Implementation using Planer Technique", *Proceedings of International Conference on Physical Sciences*. 2020.

[16] L. Martinez, "Compact Folded Bandpass Filter in Empty Substrate Integrated Coaxial Line at $ S $-Band", *IEEE Microwave and Wireless Components Letters*, Vol. 29, No. 5, pp. 315-317, 2019.

[17] Haq Tanveerul, "Extremely Sensitive Microwave Sensor for Evaluation of Dielectric Characteristics of Low-Permittivity Materials", *Sensors*, Vol. 20, pp. 1916-1926, 2020.

[18] John W. Welch, "Considerations for Two-Tier Thermal Testing of Spacecraft Electronic Units", *Proceedings of IEEE International Conference on Environmental Systems*, pp. 1-6, 2014.

[19] Jae Yoon Myung and Sang-Won Yun, "Design of a Triple-Mode Bandpass Filter using a Closed Loop Resonator", *Journal of Electromagnetic Engineering and Science*, Vol. 17, No. 2, pp. 86-90, 2017.

[20] J.T. Kuo and Chih Yuan Tsai, "Periodic Stepped-Impedance Ring Resonator (PSIRR) Bandpass Filter with a Miniaturized Area and Desirable Upper Stopband Characteristics", *IEEE Transactions on Microwave Theory and Techniques*, Vol. 54, No. 3, pp. 1107-1112, 2006.

[21] S. Aiswarya, "Analysis and Design of Stub Loaded Closed Loop Microstrip Line Filter for Wi-Fi Applications", *Proceedings of IEEE International Conference on Wireless and Optical Communication Networks*, pp. 1-14, 2019.

[22] Xuehui Guan, "A Novel Triple-Mode Bandpass Filter based on a Dual-Mode Defected Ground Structure Resonator and a Microstrip Resonator", *International Journal of Antennas and Propagation*, Vol. 23, pp. 1-14, 2013.

[23] Wu Shuang and Li Jiu Sheng, "A Novel Bandpass Filter with Dual-Mode Open-Loop Resonators", *Proceedings of IEEE International Symposium on Microwave, Antenna, Propagation, and EMC Technologies*, pp. 1-8, 2017.

[24] Lakshman Athukorala and Djuradj Budimir, "Compact Dual-Mode Open Loop Microstrip Resonators and Filters", *IEEE Microwave and Wireless Components Letters*, Vol. 19, No. 11, pp. 698-700, 2009.

[25] Xin Kai Cheng and Min Zhang, "Miniature Dual-Mode Bandpass Filters using Hexagonal Open-Loop Resonators with E-Shaped Stubs Loading", *Proceedings of IEEE International Symposium on Signals, Systems and Electronics*, pp. 1-15, 2010.

[26] Photos Vryonides, "A Novel S-Band Bandpass Filter (BPF) with Extremely Broad Stopband", *Proceedings of IEEE European Conference on Microwave*, pp. 1-13, 2018.